



Published in final edited form as:

*Osteoarthritis Cartilage*. 2015 December ; 23(12): 2242–2251. doi:10.1016/j.joca.2015.06.009.

## Characterization of degenerative human facet joints and facet joint capsular tissues

Jae-Sung Kim<sup>1,9</sup>, Mir H. Ali<sup>2</sup>, Frank Wydra<sup>1</sup>, Xin Li<sup>1</sup>, John L. Hamilton<sup>1</sup>, Howard S. An<sup>2</sup>, Gabriella Cs-Szabo<sup>1,2</sup>, Steven Andrews<sup>3</sup>, Mario Moric<sup>4</sup>, Guozhi Xiao<sup>1,5</sup>, James H-C Wang<sup>6</sup>, Di Chen<sup>1</sup>, John M. Cavanaugh<sup>7</sup>, and Hee-Jeong Im<sup>1,2,8,10,11,\*</sup>

Jae-Sung Kim: js\_kim@chosun.ac.kr; Mir H. Ali: mali@rocsc.com; Frank Wydra: fwydra@gmail.com; Xin Li: Xin\_Li@rush.edu; John L. Hamilton: John\_L\_Hamilton@rush.edu; Howard S. An: Howard\_An@rush.edu; Gabriella Cs-Szabo: Gabriella\_Cs-Szabo@rush.edu; Steven Andrews: Steve.Andrews@arraybiopharma.com; Mario Moric: Mario\_Moric@rush.edu; Guozhi Xiao: Guozhi\_Xiao@rush.edu; James H-C Wang: Wanghc@pitt.edu; Di Chen: Di\_Chen@rush.edu; John M. Cavanaugh: jmc@wayne.edu; Hee-Jeong Im: Hee-Jeong\_Sampen@rush.edu

<sup>1</sup>Department of Biochemistry, Rush University at Rush University Medical Center, Chicago, IL 60612, USA

<sup>2</sup>Department of Orthopedic Surgery, Rush University at Rush University Medical Center, Chicago, IL 60612, USA

<sup>3</sup>Array BioPharma, Boulder CO 80301, USA

<sup>4</sup>Department of Anesthesiology, Rush University at Rush University Medical Center, Chicago, IL 60612, USA

<sup>5</sup>Department of Biology and Shenzhen Key Laboratory of Cell Microenvironment, South University of Science and Technology of China, Shenzhen, 518055, China

<sup>6</sup>MechanoBiology Laboratory Departments of Orthopaedic Surgery, Bioengineering, and Mechanical Engineering and Materials Science, University of Pittsburgh, Pittsburgh, PA 15213, United States

<sup>7</sup>Bioengineering Center, Wayne State University, Detroit, MI 48202, USA

<sup>8</sup>Department of Internal Medicine, Section of Rheumatology, Rush University at Rush University Medical Center, Chicago, IL 60612, USA

\*Address correspondence to: Dr. Hee-Jeong Im Sampen, Rush University Medical Center, Cohn Research BD 516, 1735 W. Harrison St., Chicago, IL 60612, Tel: 312-942-3091, Fax: 312-942-3053, Hee-Jeong\_Sampen@rush.edu.

### Author contributions

1. The conception and design of the study, or acquisition of data, or analysis and interpretation of data: JS Kim, MH Ali, F Wydra, X Li, HS An, G Cs-Szabo, D Chen, S Andrews, JM Cavanaugh, G Xiao, JL Hamilton, M Moric, HJ Im
2. Drafting the article or revising it critically for important intellectual content: JS Kim, F Wydra, JL Hamilton, M Moric, HJ Im
3. Final approval of the version to be submitted: HJ Im

### Competing interest statement

The authors have no professional relationships with companies or manufacturers who will benefit from the results of the present study.

**Publisher's Disclaimer:** This is a PDF file of an unedited manuscript that has been accepted for publication. As a service to our customers we are providing this early version of the manuscript. The manuscript will undergo copyediting, typesetting, and review of the resulting proof before it is published in its final citable form. Please note that during the production process errors may be discovered which could affect the content, and all legal disclaimers that apply to the journal pertain.

<sup>9</sup>The Division of Natural Medical Sciences, College of Health Science, Chosun University, Gwangju, 501-759, Republic of Korea

<sup>10</sup>Department of Bioengineering, University of Illinois, Chicago, IL 60612, USA

<sup>11</sup>Jesse Brown Veterans Affairs, Chicago IL 60612, USA

## SUMMARY

**Objective**—Lumbar facet joint degeneration (FJD) may be an important cause of low back pain (LBP) and sciatica. The goal of this study was to characterize cellular alterations of inflammatory factor expression and neovascularization in human degenerative facet joint capsular (FJC) tissue, defined as the fibrous connective tissue lined with synovium that surrounds the joint. The role of these alterations in FJC tissues in pain stimulation was also assessed.

**Design**—Lumbar facet joints (FJs) were obtained from consented patients undergoing spinal reconstruction surgery and cadaveric donors with no medical history of back pain. Histological analyses of the FJ were performed to assess general structure, cellular morphology, and proteoglycan content; immunohistochemistry was used to reveal inflammatory factors and neovascularization. Cytokine antibody array and quantitative real-time polymerase chain reaction (qPCR) were used to determine the production of multiple pro- and anti-inflammatory cytokines, and western blotting (WB) was used to assay for cartilage-degrading enzymes and pain mediators. Studies using ex vivo rat dorsal root ganglion (DRG) co-culture with human FJC tissues were also performed.

**Results**—Increased neovascularization, infiltration of inflammatory cells, and pain-related axonal-promoting factors were observed in degenerative FJC tissues surgically obtained from symptomatic subjects; this was not seen in normal donor tissues. Increased angiogenic factor, VEGF, axonal promoting factor (NGF/TrkA) and sensory neuronal distribution were also detected in degenerative FJC tissues from subjects with LBP. qPCR and WB results demonstrated highly upregulated inflammatory cytokines, pain mediators, and cartilage-degrading enzymes in degenerative FJCs compared to normal. The DRG and FJC tissue ex vivo co-culture results demonstrated that degenerative FJCs from subjects reporting severe LBP altered the functional properties of DRG sensory neurons, as reflected by the increased expression of inflammatory pain molecules.

**Conclusion**—Degenerative FJC tissues possess greatly increased inflammatory and angiogenic features, suggesting that these factors play an important role in the progression of FJD and serve as a link between joint degeneration and neurological stimulation of afferent pain fibers.

## Keywords

human facet joint capsular tissue; low back pain; inflammatory cytokines; angiogenesis; nerve ingrowth; inflammatory pain mediators

## Introduction

Back pain ranks among the most common medical conditions afflicting American adults. The lifetime prevalence is about 70–85%, with 10–20% experiencing chronic low back pain

(LBP) [1]. Facet joint degeneration (FJD) as a source of LBP is often called ‘facet joint syndrome’. FJD arising from osteoarthritic changes, which is a common cause of LBP with an incidence of 15–45% among patients with chronic LBP [2–6], has been extensively reviewed in recent articles [7, 8].

Facet joints (FJs) are paired zygapophyseal joints between two consecutive vertebrae. The paired FJs and their corresponding intervertebral disc comprise a ‘three-joint complex’ constituting a ‘spinal motion segment’ [7]. FJs are subject to compressive, shear, and axial loading at the spinal motion segment. FJD may be associated with intervertebral disc degeneration [9–12]. The FJ consists of hyaline cartilage, menisci, synovium, and joint capsule. The medial branch of the dorsal primary ramus courses through the FJ and distributes sensory innervation. The human facet joint capsular (FJC) tissue, defined as the fibrous connective tissue lined with synovium surrounding the joint, is richly innervated with nociceptive nerve fibers, autonomic nerve fibers and mechanoreceptors [13–15]. Additionally, the FJ lies in close proximity to the dorsal root ganglion (DRG). [16].

Cytokine mediators of inflammation, angiogenesis, sensory neuron ingrowth and pain have been implicated as participants in joint degeneration [17–20]. Pathologic loading, which has been associated with the production of cytokines associated with inflammation, angiogenesis, sensory neuron ingrowth and pain in joint tissues [21–23], is associated with FJD [24, 25]. Studies have shown that LBP may result from facet hypertrophy, inflammation, or degradation; however, the precise relationship between FJC tissues and LBP is not completely understood [26–29].

Previous studies have demonstrated cytokine release from degenerative FJs and that the levels released are proportional to the LBP symptoms of patients [30, 31]. Other joints, such as the knee, have been shown to exhibit neovascularization in association with degeneration. Angiogenesis and associated nerve growth are linked to joint degeneration and pain [17–20]; its underlying mechanisms contributing to FJD require further study. The mechanisms by which FJD progresses to pain formation remain unclear and are the subject of continued investigation.

The goal of this study is to investigate the inflammation, angiogenesis, neuronal ingrowth and pain mediators that occur in FJC tissues obtained from subjects with chronic LBP with degenerative FJs. Additionally, to study functional mechanisms and potential cellular communication between peripheral tissues and sensory neurons, an *ex vivo* organ co-culture system using degenerative FJC tissues and rat lumbar DRGs was developed.

## Methods

### Human spine tissue acquisition

**Donor tissues**—Consented asymptomatic organ donor tissue samples were obtained from the Gift of Hope Tissue Network (Elmhurst, Illinois) within 24 hrs of death. The Gift of Hope Tissue Network provided clinical information about the organ donors from hospital charts and personal history from next of kin. Lumbar spine segments from those donors with no reported clinical back pain symptoms were harvested for our experiments. Each lumbar

segment was examined by magnetic resonance imaging (MRI). Intact FJs were removed and processed aseptically. FJC tissues were harvested and the cartilage was visually graded for degeneration from grade 0 (normal), 1–2 (early degeneration) to 3–4 (advanced degeneration) according to the scale developed by Collins et al. [32] in conjunction with an established MRI grading system for FJD [10].

**Surgical tissues**—After obtaining Institutional Review Board (IRB) approval and patient consent, intact FJs were removed from patients with LBP undergoing routine spinal fusion and supplied to us by the Orthopedic Tissue Repository. The FJs were then graded as described above. Tissue sources and detailed tissue information are listed in Table 1.

### Western blotting

Total protein from human FJC tissues was extracted using cell lysis buffer (Cell Signaling, Danvers, MA, USA), following the instructions provided by the manufacturer. Protein concentrations of human FJC tissues were determined by the bicinchoninic acid protein assay (Pierce, Rockford, IL, USA). Equal amounts of protein (30 µg protein/well) were separated by 10% SDS-PAGE and then electroblotted onto nitrocellulose membranes for western blot analyses. Immunoreactivity was visualized using the ECL system (Amersham Biosciences, Piscataway, NJ, USA).

### Reverse transcription and real-time polymerase chain reaction

Total RNA was isolated using Trizol reagent (Invitrogen, Carlsbad, CA, USA), following the instructions provided by the manufacturer. Reverse transcription (RT) was carried out with 1 µg total RNA, using the ThermoScript™ RT-PCR system (Invitrogen) for first strand cDNA synthesis. For real-time PCR, cDNA was amplified using the MyiQ Real-Time PCR Detection System (Bio-Rad Hercules, CA, USA). A threshold cycle (Ct value) was obtained from each amplification curve using iQ5 Optical System Software provided by the manufacturer (Bio-Rad). Relative mRNA expression was determined using the  $2^{-Ct}$  method, as detailed by manufacturer (Bio-Rad). The primer sequences and their conditions will be provided upon request.

### Cytokine antibody array and quantification

An array for cytokine proteins (Cytokine Array, RayBio, Norcross, GA, USA) was used to determine alterations in cytokine levels. For the microarray assay, the directions provided by the manufacturer were precisely followed. Briefly, the membranes were incubated with 2 mL of a 1X blocking buffer at room temperature for 30 min to block membranes. After decanting the blocking buffer, the membranes were incubated overnight at 4°C with either 500 µg total protein extracted from asymptomatic donor controls (FJ grade 0 or 1 with no sign of capsular hypertrophy) or surgical FJC tissues from subjects with symptomatic LBP, followed by biotin-conjugated antibodies. After decanting, all membranes were washed three times with 2 mL of 1X wash buffer I at room temperature for 5 min, followed by washing twice more with 1X wash buffer II at room temperature. Then, all membranes were incubated with a dilution (1:250) of biotin-conjugated antibodies at room temperature for 2 hrs, and the washing steps were repeated. To visualize and measure the immunoreactivity, these membranes were further incubated with horseradish-peroxidase (HRP)-conjugated

streptavidin. Immunoreactivity was visualized using the ECL system (Amersham Biosciences, Piscataway, NJ, USA) and the Signal Visual Enhancer system (Pierce) to magnify the signal intensity. Densitometric measurements were performed by calculating the integrated density values (area relative intensity) for each spot using the Molecular Imager Versadoc MP 4000 System (Bio-Rad) and Quantity One-4.5.0 Basic 1-D Analysis Software (Bio-Rad). The positive control signals of each membrane were used to normalize signal intensity.

### **Histological/Immunohistological assessments**

Human lumbar FJs were fixed in 4% paraformaldehyde for 72 hrs, and decalcified in a 22% formic acid and 10% citric acid solution, changed every 4 days until the bone tissues were soft. The decalcified FJ tissues were cut in the transverse plane and paraffin-embedded. Serial FJ sections, exactly 5  $\mu$ m thick, were cut to prepare slides. Safranin-O Fast Green staining was used to assess general morphology and loss of proteoglycan in the cartilage ground substance. Alcian Blue Hematoxylin/Orange G staining was used to assess general morphology and structural changes. The following primary antibodies were used for immunohistochemical (IHC) staining: anti-vascular endothelial growth factor (VEGF) (ab39250; Abcam, Cambridge, MA, USA);  $\alpha$ -smooth muscle actin ( $\alpha$ -SMA) (ab5694, Abcam); CD11b (Santa Cruz Biotechnology, Dallas, TX, USA); neurofilament-M (NF-M) (Thermo Scientific, Waltham, MA, USA); and nerve growth factor (NGF)/tropomyosin receptor kinase A (TrkA) (Abcam). IHC was carried out using the standard avidin-biotin-peroxidase complex technique. Sections were then visualized using the Vectastain Kit (Vector Laboratories, Burlingame, CA, USA), followed by counterstaining with Hematoxylin. For immunofluorescence staining, a fluorescent-labeled secondary antibody was added and slides were incubated at room temperature for 1 hr in darkness. Sections were rinsed in phosphate-buffered saline (PBS), mounted in anti-fading mounting media (Vector Laboratories), and examined using an Olympus BX43 upright microscope (Olympus Optical, Center Valley, PA, USA).

### **DRG co-culture**

Adult Sprague-Dawley rats (250–300 g) without pain symptoms were euthanized with carbon dioxide. Bilateral lumbar DRGs from L1 to L5 (10 DRGs per rat) were carefully removed by aseptic dissection under stereoscopic microscopy, with particular care taken to avoid physical damage. Three randomly selected rat DRGs were placed into individual wells and co-cultured in DMEM media containing 1% mini-ITS, 1% GlutaMAX, and 1% HEPES for 5 days with normal or degenerative FJC tissues or media control. Each experimental group comprised 3 wells with media control, or unique normal or degenerative FJC tissues in each well. The 3 DRGs in each well were harvested for RNA extraction and PCR as previously described [33].

### **Statistical analysis**

SPSS for Windows (Version 12.0, IBM Corporation, Somers, NY) and SAS (version 9.2, SAS Institute, Cary, NC) were used to calculate descriptive statistics, to test group differences and to correct for error inflation due to multiple testing. For variables that have approximately normal distributions and similar variances, a two-sided t-test was used to

compare groups. To adjust for the problem of error inflation due to multiple hypothesis testing we used an adjustment method to control the false discovery rate (FDR) as described by Benjamini and Hochberg (1995)[34]. The P-values, grouped by analytical section, were adjusted using linear step-up adjustments in a manner that controls the FDR, hence minimizing issues of error inflation. A  $p < 0.05$  significance level, after adjustment for error inflation, was used for all statistical tests. Individual  $p$ -values represented in the figures. Data represented as mean. Error bars represented as 95% confidence interval (CI).

## Results

### Gross and histologic appearance of human FJD

Gross appearances of human FJs were examined and assigned a representative grade for the appearance of the inferior facet (Collin's grades: G0–G4; Figure 1A&B) [32, 35]. Samples with higher grades showed an increase in the size of edge osteophytes, reactive bone, and cartilage eburnation. The symptomatic surgical samples clearly had the most degenerative morphological changes (Table 1). The gross appearance of human FJs was further analyzed by histological examination for proteoglycan content by comparing normal (G0) with degenerated facets with different grades of pathological conditions (G2–4). Safranin O staining revealed severe depletion of proteoglycan in facet joints with advanced degeneration (G3/4) compared to normal joints (G0) (Figure 1C). Alcian Blue Hematoxylin/Orange G and H&E staining results of the FJs further supported observations of the structural and morphological changes correlated with grade (Figure 1D&E).

### Inflammation is increased in degenerative FJC tissues

Results of staining for CD11b, a marker of immune cell infiltration, indicated infiltration of inflammatory cells in degenerative FJC tissues (Figure 2A). We examined the expression of cytokines in degenerative FJC tissues (G3/4) compared to normal FJC tissues (G0). Results from cytokine antibody array analyses revealed a significant increase in the levels of multiple pro-inflammatory cytokines, including GRO $\alpha$ , sICAM-1, INF- $\gamma$ , IL-1 $\beta$ , IL-17, RANTES and TNF $\alpha$  ( $p < 0.01$ ) and IL-1 $\alpha$ , IL-17E ( $p < 0.05$ ), as well as an increase in the level of anti-inflammatory cytokines IL-10 and IL-13 ( $p < 0.05$ ) (Figure 3A).

Quantitative real-time PCR (qPCR) analysis was employed to support the cytokine antibody array data. The results demonstrated that the induced protein levels correlated with increased mRNA levels of pro-inflammatory cytokines (Figure 3B). Our individual qPCR data revealed slight differences between mRNA and protein levels assessed by the cytokine antibody array. For example, we did not observe significant upregulation of IL-8, CCL2, and IL-1Ra at the protein level, but RNA levels were significantly increased in degenerative FJC tissues ( $p < 0.05$ ) (Figure 3B). qPCR analyses also found significant upregulation of additional pro- and anti-inflammatory cytokines that were not analyzed in the cytokine assay system, including IL-18 and IL-11, and toll-like receptors TLR2 and TLR4 ( $p < 0.05$ ) (Figure 3B).

### **Neovascularization is increased in degenerative FJC tissues**

Markedly increased neovascularization was evident in the degenerative FJC tissues, as assessed by immunoreactivity for  $\alpha$ -SMA (Figure 2B). When comparing normal (G0) or early FJ degeneration (G1) with advanced degenerative FJC tissues (G3/4), neovascularization was clearly increased. These angiogenic events correlated with an increase in VEGF expression, assessed by immunohistochemistry (Figure 2C; upper panel) and western blot analyses (Figure 2C; lower panel).

### **Neurogenesis is increased in degenerative FJC tissues**

In the advanced stage of degenerative FJC tissues (G3/4) compared to normal (G0) or early stage of degenerative tissues (G1), IHC results demonstrated that neurofilament-M (NF-M; a marker of neurite formation) was substantially increased (Figure 2D). Correspondingly, our results revealed that the NGF/TrkA axis is highly upregulated in the advanced degenerative stage of FJC tissues, as assessed by IHC (Figure 2E&F), as well as by qPCR analyses for mRNA levels of NGF and TrkA ( $p < 0.01$ ) (Figure 5C).

### **Degenerative FJC tissues overexpress cartilage-degrading enzymes and tissue inhibitors of metalloproteinases (TIMPs)**

We examined levels of key cartilage-degrading matrix metalloproteinases (MMPs) and aggrecanases, such as MMP-13, MMP-1, MMP-3, ADAMTS-4 and ADAMTS-5, by comparing normal with degenerative FJC tissues. Collagenases (MMP-1, MMP-13) and stromelysin (MMP-3) were highly upregulated in degenerative FJC tissues at both mRNA (Figure 4A,  $p < 0.01$ ) and protein levels (Figure 4A'). Similarly, critical aggrecanases, ADAMTS-4 and ADAMTS-5, were significantly increased at both mRNA (Figure 4B,  $p < 0.05$ ) and protein levels (Figure 4B'). Modulation of gene expression was not limited to cartilage-degrading enzymes; we also observed striking induction of tissue inhibitors of metalloproteinases (TIMPs), family members that antagonize cartilage-degrading enzyme activities in the degenerative FJC tissues. These included TIMP-2 and TIMP-3 at mRNA (Figure 4C,  $p < 0.05$ ) and protein levels (Figure 4C'). We did not observe a significant increase in TIMP-1 in degenerative FJC tissues (Figure 4C).

### **Degenerative FJC tissues overexpress pain-related molecules and influence the expression of pain mediators in sensory neurons in an ex vivo DRG organ co-culture model**

We further examined whether FJC tissues from degenerative FJs overexpress pain-related molecules. Our real-time PCR and western blotting analyses revealed significant increases in both mRNA and protein levels in inflammatory pain mediators inducible nitric oxide synthase (iNOS) and cyclooxygenase-2 (COX-2) (Figure 5A,  $p < 0.05$ ). Among the subtypes of prostaglandin receptors, expression levels of EP<sub>1</sub>, EP<sub>3</sub> and EP<sub>4</sub> were significantly ( $p < 0.05$ ) elevated in degenerative FJC tissues (G3/4) compared to normal (G0). Unexpectedly, the level of EP<sub>2</sub> was reduced in degenerative FJC tissues compared to normal at both mRNA ( $p < 0.05$ ) and protein levels (Figure 5B).

Significant increases in expression of neuromodulators, including substance P, calcitonin gene-related peptide (CGRP), NGF, TrkA, and pain-associated ion channel transient

receptor potential cation channel subfamily V member 1 (TRPV1), were found in degenerative compared to normal FJC tissues (Figure 5C;  $p < 0.05$  or  $p < 0.01$ ). Our DRG co-culture model revealed that degenerative FJC tissues significantly altered the production of pain mediators in DRGs, reflected by the overexpression of substance P ( $p < 0.05$ ) and NGF ( $p < 0.01$ ; Figure 5D).

## Discussion

Our results revealed that FJC tissues harvested from degenerative FJs from subjects with LBP displayed higher levels of angiogenesis, inflammation, and neurogenesis when compared to healthier FJC tissues harvested from asymptomatic donors. Additionally, degenerated FJC tissues greatly overexpressed pain-related molecules that may prompt DRG neurons to increase pain sensitization.

Elevated levels of pro-inflammatory cytokines, as well as cartilage-degrading enzymes, seen in degenerative FJs (G3/4) compared to normal FJs (G0) strongly support the proposition that these molecules play roles in structural and molecular changes in FJC tissues and in adjacent FJs. Nevertheless, it must be noted that not only pro-inflammatory cytokines and cartilage-degrading enzymes, but also anti-inflammatory cytokines and inhibitors of cartilage-degrading enzymes, including IL-10, IL-13, TIMP-2 and TIMP-3, are upregulated in parallel. Similar observations have been noted in other human joint structural tissues, suggesting that this may be an unsuccessful attempt of the reparative response to overcome the degenerative process [36–38].

Recent studies have implicated angiogenesis as having a principal role in the development of joint degenerative disease and pain through stimulation of inflammation and innervation [39–41]. It has been suggested that the influx of inflammatory cells into the joint resulting from angiogenesis may exacerbate degeneration and lead to LBP [42, 43]. Angiogenesis, itself, promotes the ingrowth of new sensory nerve fibers and is a possible cause of enhanced pain perception [17, 18, 20]. An upregulation of angiogenic factors, inflammatory cytokines, immune cell infiltration, and newly formed sensory nerve fiber ingrowth within the FJC of symptomatic patients may be indicative of a progressive pattern leading from the initiation of FJ degeneration to pain production.

Newly formed sensory nerve fibers found in degenerative FJs respond to inflammation and, additionally, initiate or facilitate inflammation through the release of vasoactive substances into the joint [44–46]. The close proximity of the FJ to the DRG may enhance these “crosstalk” capabilities. Damage to the FJ leads to the release of inflammatory cytokines and pain-mediators by sensory neurons in the DRGs; consequently, these released molecules become critical compounding factors in nociceptive changes in degenerative FJs [47, 48]. Our DRG co-culture model demonstrates that degenerative FJC tissues modify the functional properties of sensory neurons in the DRG, as seen by the overproduction of the critical pain mediators substance P and NGF. Our results suggest that “crosstalk” between the degenerated FJ and DRG, in combination with the upregulation of inflammatory neuropeptides, receptors, and ion channels (e.g., substance P, COX-2, CGRP, EP receptors, TRPV1 and the NGF/TrkA axis) exacerbate pain production in symptomatic LBP patients.



We previously reported that TIMP-3, the most potent chondroprotective molecule among the four TIMP family members (TIMP1~4), is significantly reduced in osteoarthritic knee cartilage compared to normal knee cartilage [49]. However, in the present study, we observed that TIMP-3 is one of the molecules that was greatly increased in degenerative FJC tissues compared to normal. In addition, we also found a significant reduction in prostaglandin E2 receptor EP<sub>2</sub> in degenerative FJC tissues. The EP<sub>2</sub> receptor is highly upregulated in degenerative knee joint cartilage, and is known to be linked to the pathophysiology of cartilage [50]. These results suggest there may be tissue-specific differential expression patterns of these molecules.

While this study produced important results, there are limitations that must be considered. First, limitations may exist due to the small sample size, especially for normal tissues (G0). Obtaining a large sample population proved difficult because samples were acquired surgically from consented patients or from cadaveric organ donors. Second, there was limited personal information available from the cadaveric donors because pain scores directly resulting from LBP were not available. Third, there may be incongruities in the DRG co-culture model because of the use of rat DRGs with human FJC tissues. Continuing studies using the DRG co-culture system to examine other targets should prove beneficial to the understanding of “crosstalk” between peripheral tissues and the sensory nerve system.

In summary, our data suggest that increased inflammatory and angiogenic features in degenerative FJC tissues play an important role in the progression of FJD and serve as a link between joint degeneration and neurological stimulation of afferent pain fibers. Reproducing symptomatic FJD leading to FJ pain in animal models will greatly enhance our understanding of translational or pre-clinical information that cannot be answered from human clinical studies.

## Acknowledgments

This work was supported by NIH R01 grants AR053220, AR062136 (to HJJ) and AR05947 (to GX) as well as a VA BLD&R Merit Award I01BX002647 (to HJJ), the National Natural Science Foundation of China Grant (81472049 to GX), and the National Research Foundation of Korea-2012R1A1A2005306 (to JSK). We thank the Gift of Hope Organ Tissue Donor Network as well as Drs. Chubinskaya and Margulis for making human tissues available, and we also extend our appreciation to the family members of the tissue donors who made it possible.

### Role of the funding source

The study sponsor had no involvement in the study design, collection, analysis and interpretation of data, writing of the manuscript and decision to submit the manuscript for publication. This study was supported by NIH NIAMS R01 grants from AR053220 (to HJJ), AR062136 (to HJJ) and AR05947 (to GX) as well as VA BLD&R Merit Review Award (to HJJ), the National Research Foundation of Korea-2012R1A1A2005306 (to JSK) and the National Natural Science Foundation of China Grant (81472049 to GX).

## References

1. Andersson GB. Epidemiological features of chronic low-back pain. *Lancet*. 1999; 354:581–585. [PubMed: 10470716]
2. Schwarzer AC, Aprill CN, Derby R, Fortin J, Kine G, Bogduk N. Clinical features of patients with pain stemming from the lumbar zygapophysial joints. Is the lumbar facet syndrome a clinical entity? *Spine (Phila Pa 1976)*. 1994; 19:1132–1137. [PubMed: 8059268]

3. Schwarzer AC, Wang SC, Bogduk N, McNaught PJ, Laurent R. Prevalence and clinical features of lumbar zygapophysial joint pain: a study in an Australian population with chronic low back pain. *Ann Rheum Dis.* 1995; 54:100–106. [PubMed: 7702395]
4. Moran R, O'Connell D, Walsh MG. The diagnostic value of facet joint injections. *Spine (Phila Pa 1976).* 1988; 13:1407–1410. [PubMed: 3212574]
5. Manchikanti L, Boswell MV, Singh V, Pampati V, Damron KS, Beyer CD. Prevalence of facet joint pain in chronic spinal pain of cervical, thoracic, and lumbar regions. *BMC Musculoskelet Disord.* 2004; 5:15. [PubMed: 15169547]
6. Dreyer SJ, Dreyfuss PH. Low back pain and the zygapophysial (facet) joints. *Arch Phys Med Rehabil.* 1996; 77:290–300. [PubMed: 8600875]
7. Gellhorn AC, Katz JN, Suri P. Osteoarthritis of the spine: the facet joints. *Nat Rev Rheumatol.* 2013; 9:216–224. [PubMed: 23147891]
8. Cohen SP, Huang JH, Brummett C. Facet joint pain—advances in patient selection and treatment. *Nat Rev Rheumatol.* 2013; 9:101–116. [PubMed: 23165358]
9. Butler D, Trafimow JH, Andersson GB, McNeill TW, Huckman MS. Discs degenerate before facets. *Spine (Phila Pa 1976).* 1990; 15:111–113. [PubMed: 2326704]
10. Fujiwara A, Tamai K, Yamato M, An HS, Yoshida H, Saotome K, et al. The relationship between facet joint osteoarthritis and disc degeneration of the lumbar spine: an MRI study. *Eur Spine J.* 1999; 8:396–401. [PubMed: 10552323]
11. Suri P, Miyakoshi A, Hunter DJ, Jarvik JG, Rainville J, Guermazi A, et al. Does lumbar spinal degeneration begin with the anterior structures? A study of the observed epidemiology in a community-based population. *BMC Musculoskelet Disord.* 2011; 12:202. [PubMed: 21914197]
12. Eubanks JD, Lee MJ, Cassinelli E, Ahn NU. Does lumbar facet arthrosis precede disc degeneration? A postmortem study. *Clin Orthop Relat Res.* 2007; 464:184–189. [PubMed: 17767079]
13. Cavanaugh JM, Lu Y, Chen C, Kallakuri S. Pain generation in lumbar and cervical facet joints. *J Bone Joint Surg Am.* 2006; 88 (Suppl 2):63–67. [PubMed: 16595446]
14. Ashton IK, Ashton BA, Gibson SJ, Polak JM, Jaffray DC, Eisenstein SM. Morphological basis for back pain: the demonstration of nerve fibers and neuropeptides in the lumbar facet joint capsule but not in ligamentum flavum. *J Orthop Res.* 1992; 10:72–78. [PubMed: 1530799]
15. Yamashita T, Cavanaugh JM, el-Bohy AA, Getchell TV, King AI. Mechanosensitive afferent units in the lumbar facet joint. *J Bone Joint Surg Am.* 1990; 72:865–870. [PubMed: 2365719]
16. Kalichman L, Hunter DJ. Lumbar facet joint osteoarthritis: a review. *Semin Arthritis Rheum.* 2007; 37:69–80. [PubMed: 17379279]
17. Ashraf S, Walsh DA. Angiogenesis in osteoarthritis. *Curr Opin Rheumatol.* 2008; 20:573–580. [PubMed: 18698180]
18. Mapp PI, Walsh DA. Mechanisms and targets of angiogenesis and nerve growth in osteoarthritis. *Nat Rev Rheumatol.* 2012; 8:390–398. [PubMed: 22641138]
19. Walsh DA. Angiogenesis and arthritis. *Rheumatology (Oxford).* 1999; 38:103–112. [PubMed: 10342621]
20. Walsh DA, McWilliams DF, Turley MJ, Dixon MR, Franses RE, Mapp PI, et al. Angiogenesis and nerve growth factor at the osteochondral junction in rheumatoid arthritis and osteoarthritis. *Rheumatology (Oxford).* 2010; 49:1852–1861. [PubMed: 20581375]
21. Pufe T, Lemke A, Kurz B, Petersen W, Tillmann B, Grodzinsky AJ, et al. Mechanical overload induces VEGF in cartilage discs via hypoxia-inducible factor. *Am J Pathol.* 2004; 164:185–192. [PubMed: 14695332]
22. Griffin TM, Guilak F. The role of mechanical loading in the onset and progression of osteoarthritis. *Exerc Sport Sci Rev.* 2005; 33:195–200. [PubMed: 16239837]
23. Pecchi E, Priam S, Gosset M, Pigenet A, Sudre L, Laigüillon MC, et al. Induction of nerve growth factor expression and release by mechanical and inflammatory stimuli in chondrocytes: possible involvement in osteoarthritis pain. *Arthritis Res Ther.* 2014; 16:R16. [PubMed: 24438745]
24. Brown KR, Pollintine P, Adams MA. Biomechanical implications of degenerative joint disease in the apophyseal joints of human thoracic and lumbar vertebrae. *Am J Phys Anthropol.* 2008; 136:318–326. [PubMed: 18324643]

25. Tischer T, Aktas T, Milz S, Putz RV. Detailed pathological changes of human lumbar facet joints L1–L5 in elderly individuals. *Eur Spine J*. 2006; 15:308–315. [PubMed: 16021481]
26. Jackson RP. The facet syndrome. Myth or reality? *Clin Orthop Relat Res*. 1992;110–121. [PubMed: 1534721]
27. van Kleef M, Vanelderen P, Cohen SP, Lataster A, Van Zundert J, Mekhail N. Pain originating from the lumbar facet joints. *Pain Pract*. 2010; 10:459–469. [PubMed: 20667027]
28. Varlotta GP, Lefkowitz TR, Schweitzer M, Errico TJ, Spivak J, Bendo JA, et al. The lumbar facet joint: a review of current knowledge: part I: anatomy, biomechanics, and grading. *Skeletal Radiol*. 2011; 40:13–23. [PubMed: 20625896]
29. Varlotta GP, Lefkowitz TR, Schweitzer M, Errico TJ, Spivak J, Bendo JA, et al. The lumbar facet joint: a review of current knowledge: Part II: diagnosis and management. *Skeletal Radiol*. 2011; 40:149–157. [PubMed: 20577735]
30. Igarashi A, Kikuchi S, Konno S, Olmarker K. Inflammatory cytokines released from the facet joint tissue in degenerative lumbar spinal disorders. *Spine (Phila Pa 1976)*. 2004; 29:2091–2095. [PubMed: 15454697]
31. Igarashi A, Kikuchi S, Konno S. Correlation between inflammatory cytokines released from the lumbar facet joint tissue and symptoms in degenerative lumbar spinal disorders. *J Orthop Sci*. 2007; 12:154–160. [PubMed: 17393271]
32. Collins DH. The pathology of osteoarthritis. *Br J Rheumatol*. 1939; 1:248–262.
33. Li X, Kim JS, van Wijnen AJ, Im HJ. Osteoarthritic tissues modulate functional properties of sensory neurons associated with symptomatic OA pain. *Mol Biol Rep*. 2011; 38:5335–5339. [PubMed: 21327824]
34. Benjamini Y, Hochberg Y. Controlling the false discovery rate: a practical and powerful approach to multiple testing. *J Roy Statist Soc Ser B*. 1995; 57(11):289–300.
35. Muehleman C, Bareither D, Huch K, Cole AA, Kuettner KE. Prevalence of degenerative morphological changes in the joints of the lower extremity. *Osteoarthritis Cartilage*. 1997; 5:23–37. [PubMed: 9010876]
36. Martel-Pelletier J, Alaaeddine N, Pelletier JP. Cytokines and their role in the pathophysiology of osteoarthritis. *Front Biosci*. 1999; 4:D694–703. [PubMed: 10525480]
37. Goldring MB. Osteoarthritis and cartilage: the role of cytokines. *Curr Rheumatol Rep*. 2000; 2:459–465. [PubMed: 11123098]
38. Iannone F, Lapadula G. The pathophysiology of osteoarthritis. *Aging Clin Exp Res*. 2003; 15:364–372. [PubMed: 14703002]
39. Im HJ, Kim JS, Li X, Kotwal N, Sumner DR, van Wijnen AJ, et al. Alteration of sensory neurons and spinal response to an experimental osteoarthritis pain model. *Arthritis Rheum*. 2010; 62:2995–3005. [PubMed: 20556813]
40. Yoo SA, Kwok SK, Kim WU. Proinflammatory role of vascular endothelial growth factor in the pathogenesis of rheumatoid arthritis: prospects for therapeutic intervention. *Mediators Inflamm*. 2008; 2008:129873. [PubMed: 19223981]
41. Ashraf S, Mapp PI, Walsh DA. Angiogenesis and the persistence of inflammation in a rat model of proliferative synovitis. *Arthritis Rheum*. 2010; 62:1890–1898. [PubMed: 20309868]
42. Fernandes JC, Martel-Pelletier J, Pelletier JP. The role of cytokines in osteoarthritis pathophysiology. *Biorheology*. 2002; 39:237–246. [PubMed: 12082286]
43. Sutton S, Clutterbuck A, Harris P, Gent T, Freeman S, Foster N, et al. The contribution of the synovium, synovial derived inflammatory cytokines and neuropeptides to the pathogenesis of osteoarthritis. *Vet J*. 2009; 179:10–24. [PubMed: 17911037]
44. Ahmed AS, Li J, Ahmed M, Hua L, Yakovleva T, Ossipov MH, et al. Attenuation of pain and inflammation in adjuvant-induced arthritis by the proteasome inhibitor MG132. *Arthritis Rheum*. 2010; 62:2160–2169. [PubMed: 20506183]
45. Hernanz A, De Miguel E, Romera N, Perez-Ayala C, Gijon J, Arnalich F. Calcitonin gene-related peptide II, substance P and vasoactive intestinal peptide in plasma and synovial fluid from patients with inflammatory joint disease. *Br J Rheumatol*. 1993; 32:31–35. [PubMed: 7678534]
46. Ahmed M, Bjurholm A, Schultzberg M, Theodorsson E, Kreicbergs A. Increased levels of substance P and calcitonin gene-related peptide in rat adjuvant arthritis. A combined

- immunohistochemical and radioimmunoassay analysis. *Arthritis Rheum.* 1995; 38:699–709. [PubMed: 7538298]
47. Sakuma Y, Ohtori S, Miyagi M, Ishikawa T, Inoue G, Doya H, et al. Up-regulation of p55 TNF alpha-receptor in dorsal root ganglia neurons following lumbar facet joint injury in rats. *Eur Spine J.* 2007; 16:1273–1278. [PubMed: 17468886]
48. Miyagi M, Ohtori S, Ishikawa T, Aoki Y, Ozawa T, Doya H, et al. Up-regulation of TNFalpha in DRG satellite cells following lumbar facet joint injury in rats. *Eur Spine J.* 2006; 15:953–958. [PubMed: 16758109]
49. Yan D, Chen D, Hawse JR, van Wijnen AJ, Im HJ. Bovine lactoferricin induces TIMP-3 via the ERK1/2-Sp1 axis in human articular chondrocytes. *Gene.* 2013; 517:12–18. [PubMed: 23313877]
50. Li X, Ellman M, Muddasani P, Wang JH, Cs-Szabo G, van Wijnen AJ, et al. Prostaglandin E2 and its cognate EP receptors control human adult articular cartilage homeostasis and are linked to the pathophysiology of osteoarthritis. *Arthritis Rheum.* 2009; 60:513–523. [PubMed: 19180509]

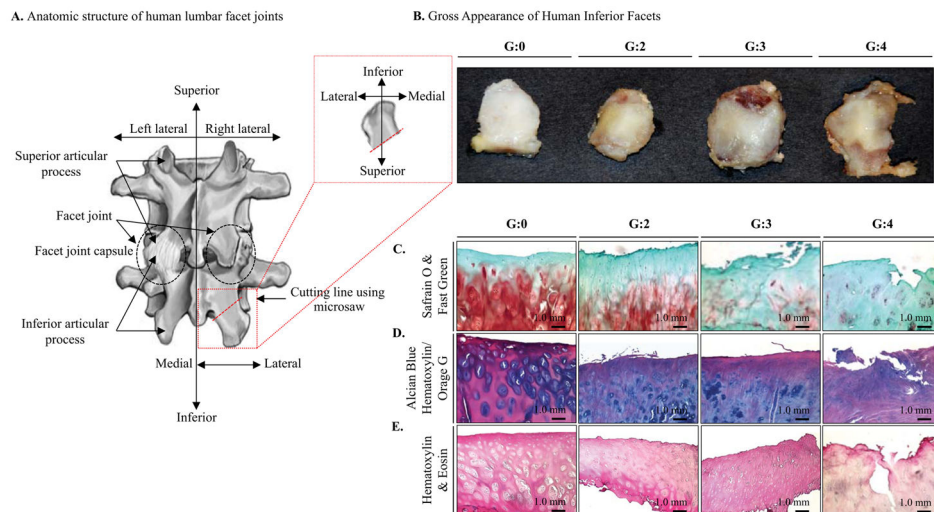


**Fig. 1. Gross and histologic appearances of normal and degenerative FJs**

A, Anatomical structure of human lumbar FJ and preparation of inferior articular process in lumbar FJ. B, Gross appearances of FJs and FJC tissues. Each FJ was assigned a representative grade for the appearance of the inferior facet. The higher graded FJ samples demonstrates an increase in the size of edge osteophytes, reactive bone, and cartilage eburnation. C, Safranin O, D, Alcian Blue Hematoxylin/Orange G, and E, Hematoxylin & Eosin staining of FJ cartilage show severe depletion of proteoglycan, fibrillation, structural and morphological changes in degenerative FJs (G4) compared to normal FJs (G0). The results represent donor number of at least n=3 for G0 and n=6 for each grades, G2-4.

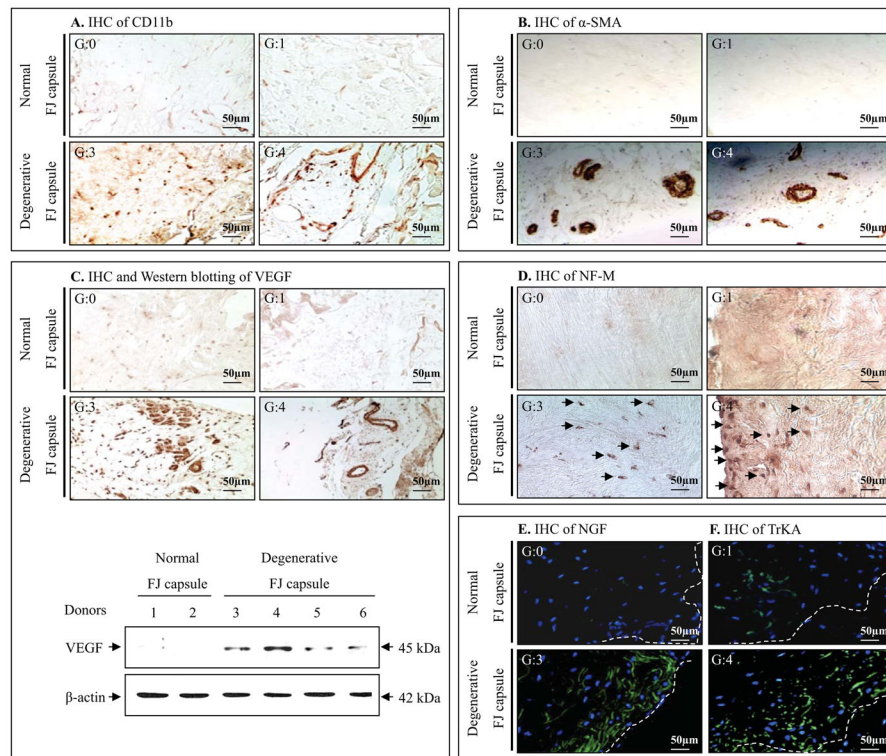


**Fig. 2. Assessment of inflammation, neovascularization, and neuron ingrowth in normal and degenerative FJC tissue**

A, Immunohistochemical (IHC) staining of CD11b indicates increased infiltration of inflammatory cells in degenerative FJC tissues (G3/4) compared to normal FJC tissues (G0). B, IHC staining of smooth muscle actin ( $\alpha$ -SMA) shows markedly increased angiogenic events in degenerative FJC (G3/4) tissues compared to normal FJC tissues (G0). C, IHC staining of VEGF (upper panel) and western blotting analyses (lower panel) show increased induction of VEGF in degenerative FJC tissue (G3/4) compared to NFJC tissues (G0). D–F, IHC results demonstrate substantially increased neuro-filament-M (NF-M; a marker of neurite formation), neuronal growth promoting factor, NGF, and its cognate receptor TrkA in degenerative FJC (G3/4) compared to normal FJC tissues (G0). These results represent at least  $n=3$  for normal FJC tissue and  $n=6$  for degenerative FJC tissue (G1~4).

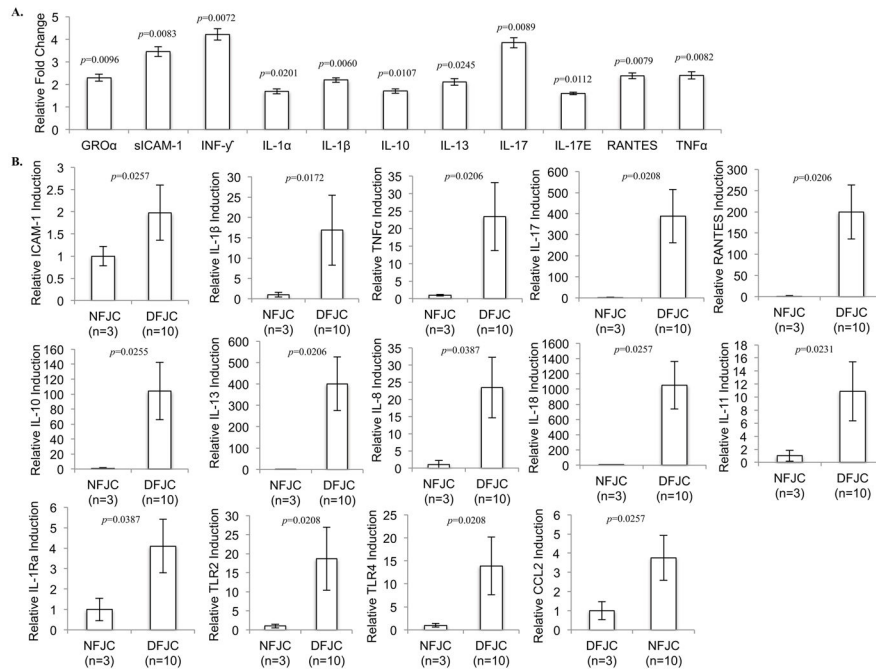


**Fig. 3. Cytokine profiling in normal and degenerative facet joint capsular (FJC) tissues**  
 A, Densitometric Analyses of Cytokine Antibody Array, using FJC tissue lysates from normal (G0) and degenerative FJ tissues (G3/4). The histogram shows levels of altered cytokines in degenerative FJC tissues (n=10) relative to normal FJC tissues (n=3). B, Quantitative real-time PCR analyses for comparative gene expression profile of pro- and anti-inflammatory cytokines and TLRs, between normal FJC tissues (G0) (NFJC, n=3) and degenerative FJC tissues (DFJC, G3/4) (n=10). Individual p-values represented in the figures. Data represented as mean. Error bars represented as 95% CI.

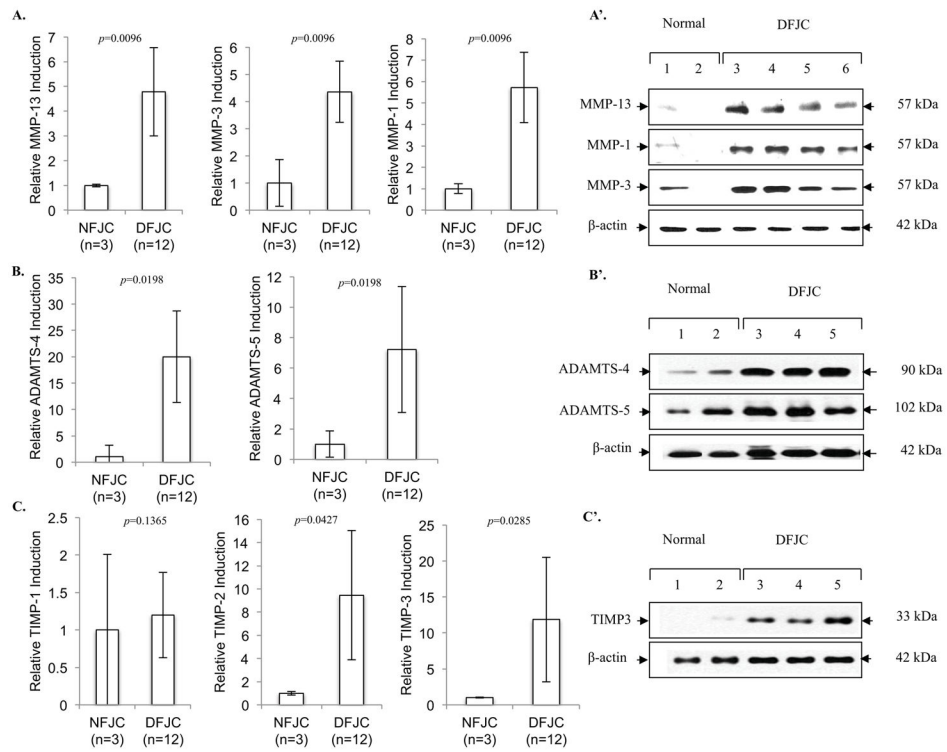


**Fig. 4. Expression of cartilage degrading enzymes and TIMPs in normal and degenerative FJC tissues**

Comparison of MMPs, ADAMTSs, and TIMPs assessed by quantitative real-time PCR for mRNA levels (A–C, n=3 normal (NFJC, G0); n=12 degenerative FJC (DFJC, G3/4) tissue) (A–C) and western blotting for protein (n=3 NFJC; n=3 DFJC) (A'–C'). Individual p-values represented in the figures. Data represented as mean. Error bars represented as 95% CI.



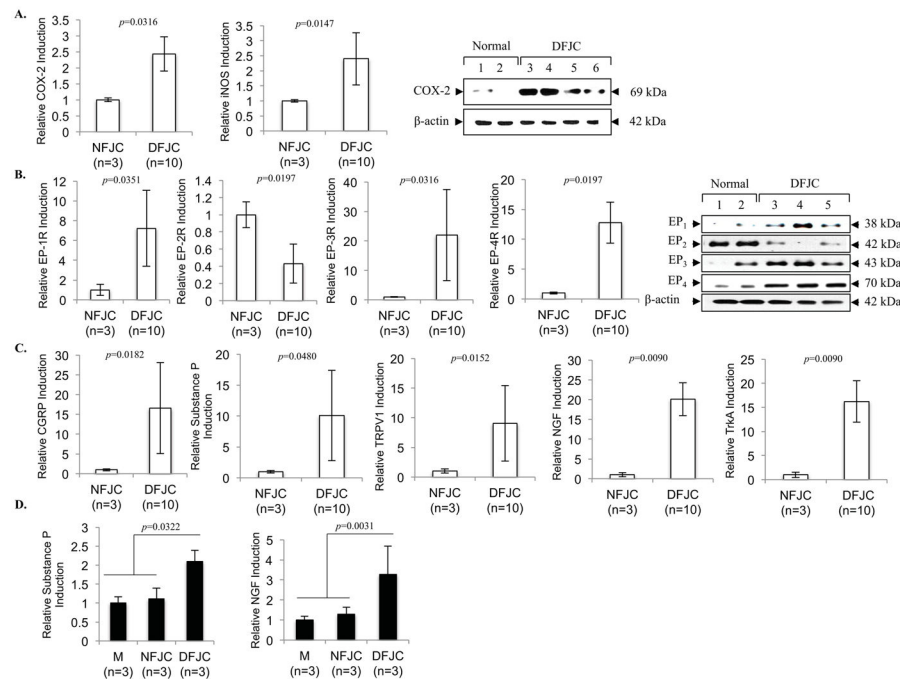


**Fig. 5. The level of inflammatory pain mediators and pain neuromodulators in normal and degenerative FJC tissues**

Comparison of A, COX-2, iNOS; B, prostaglandin (EP) receptors; and C, pain neuromodulator (CGRP, Substance P, TRPV1, NGF, TrkA) expression in degenerative FJC tissue (G3/4, DFJC) as compared to normal FJC tissue (G0, NFJC), which was assessed by quantitative real-time PCR for mRNA (n=3, NFJC; n=10 DFJC tissue) and western blotting for protein (n=3 NFJC tissue; n=3 DFJC tissue). D, isolated rat DRGs were co-cultured with media control (M), NFJC tissue, or DFJC tissue for 5 days. Assessment of total relative gene induction was assessed by quantitative real-time PCR analyses of substance P and NGF in DRGs. The data represent 3 independent experiments (n=3 donors) with triplicates. Individual p-values represented in the figures. Data represented as mean. Error bars represented as 95% CI.

**Table 1**

Demographics of collected facet joints

Sample type	Age	Gender	Symptom	FJ Grade
Clinical sample (surgically removed)	77Y	F	Osteoporosis, degenerative facets, spinal stenosis with severe back pain	G4
	82Y	M	Severe spinal stenosis, degenerative facet with severe back pain	G4
	47Y	M	Lateral recess stenosis with severe back pain	G4
	67Y	F	Degenerative scoliosis and spondylolisthesis with severe back pain	G4
	78Y	M	Spondylolisthesis, spinal stenosis, degenerative facet, severe back pain	G4
	30Y	M	Degenerative disc disease and low back pain	G3
	39Y	M	Disc degeneration with severe back pain, a traumatic low back injury	G3
	80Y	F	Degenerative spondylosis with low back pain, Degenerative facet	G4
	63Y	F	Spondylosistehsis, spinal stenosis, degenerative facets, low back pain	G4
	31Y	M	Severe low back pain	G3
	57Y	F	Degenerative lumbar scoliosis	G3
	77Y	F	Spondylolisthesis, highly degenerated facet joint	G3
	75Y	F	Spinal stenosis with bilateral leg and back pain	G4
	62Y	M	Degenerative scoliosis, L3/L4 spondylolisthesis, L3/L4 lumbar stenosis, low back pain	G4
	70Y	F	Severe low back pain, Severe facet joint degeneration	G4
	56Y	M	Severe facet joint degeneration, low back pain	G3
	74Y	F	Severe facet joint degeneration, low back pain	G3
Cadaver	61 Y	M	Loss of cartilage exposing the underlying bone, Bilateral L3/4 facet	G4
			Surface fissures to deep zone, Left L4/5 facet	G3
	21 Y	F	Intact surface, Bilateral L3/4 facet	G0
			Intact surface, Bilateral L4/5 facet	G0
	48Y	F	Surface fissure, Bilateral L3/4 facet	G1
			Surface fissure, Bilateral L4/5 facet	G1
	48Y	M	Surface fissures to deep zone, Left L4/5 facet	G3
			Surface fissures to mid zone Bilateral L4/5 facet	G2
	50Y	M	Surface fissures to mid zone, Right L4/5 facet	G2
	56Y	M	Surface fissures to deep zone, Left L3/4 facet	G3

Sample type	Age	Gender	Symptom	FJ Grade
			Complete destruction, Bilateral L4/5 facet	G4
	44Y	F	Surface fissures to mid zone Bilateral L3/4 facet	G2
			Surface fissures to mid zone Bilateral L4/5 facet	G2
	28Y	F	Intact surface, Bilateral facet L3/4	G0
			Surface fissure, Bilateral L4/5 fact	G1
	33Y	M	Surface fissures, Bilateral L3/4 facet	G1
			Surface fissures, Bilateral L4/5 facet	G2
	53Y	F	Surface fissures to deep zone, Left L3/4 facet	G3
			Surface fissures to mid zone, Left L4/5 facet	G2
	65Y	M	Complete destruction, Bilateral L4/5 facet	G4

Grading	n number	Age	Gender		Tissue type	
			Male	Female	Clinical	Cadaver
G:0	3	23.3±4	0	3	0	3
G:1	6	36±9	3	3	0	4
G:2	6	45±7	3	3	0	6
G:3	7	53±7	4	3	5	4
G:4	15	69±10	7	8	12	3
<b>Total</b>	<b>37</b>	<b>53±17</b>	<b>17</b>	<b>20</b>	<b>17</b>	<b>20</b>